Science with Spectral Distortions of the CMB - II

Primordial Distortions

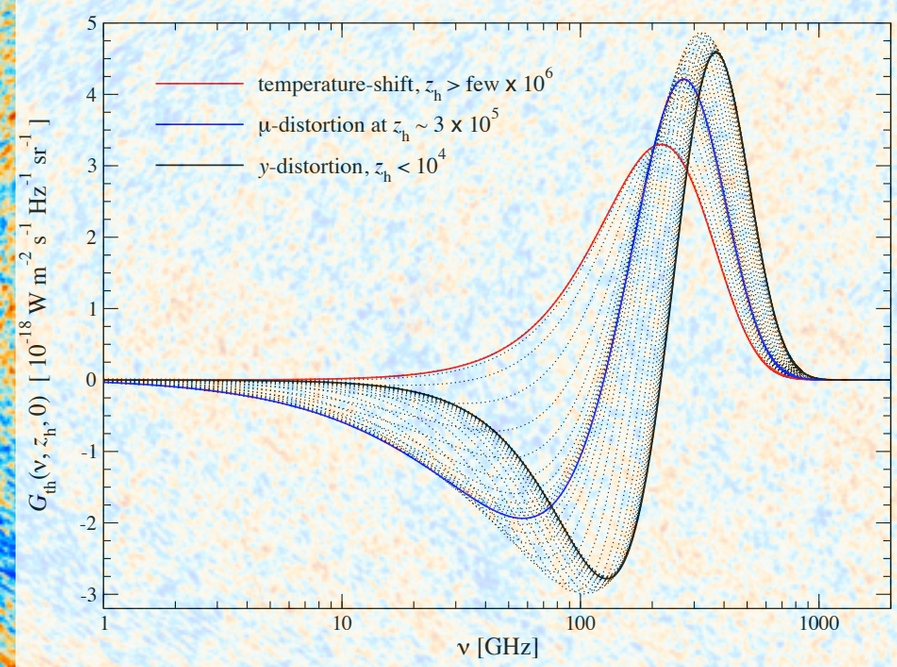

Cosmological Recombination lines

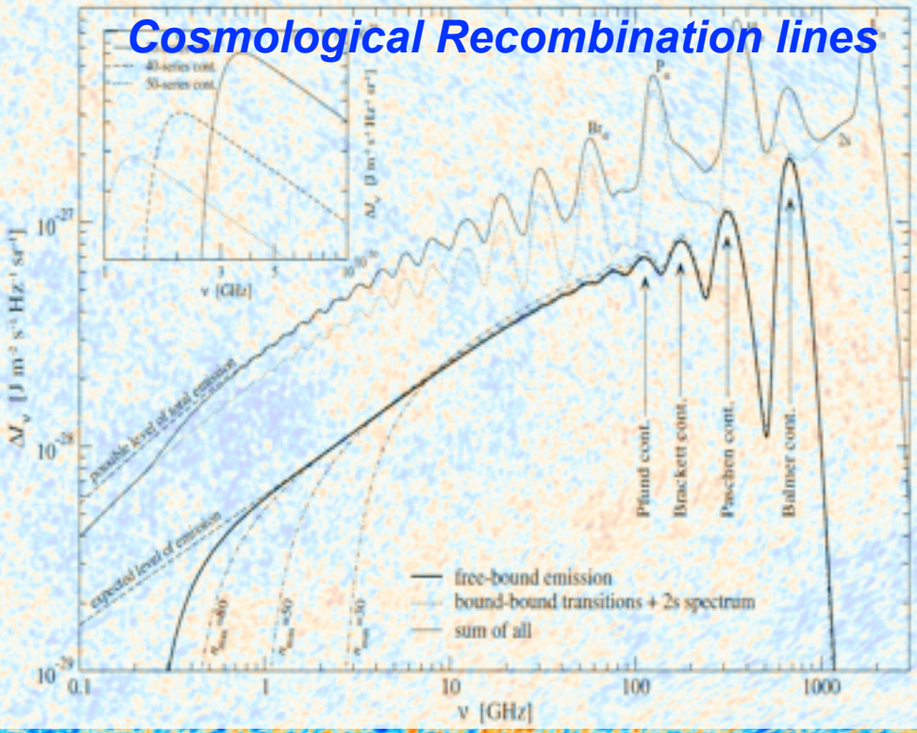

JOHNS HOPKINS UNIVERSITY

Jens Chluba

CITA ICAT Canadian Institute for Theoretical Astrophysics L'institut canadien d'astrophysique theorique

CUSO Doctoral Program in Physics

Lausanne, October 23th, 2014

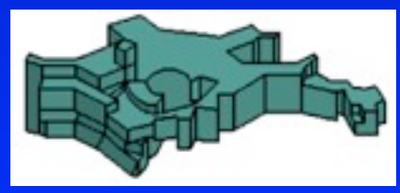

Structure of the Lectures *(at least in theory)*

Lecture I:

- Overview and motivation
- Simple blackbody radiation warm-ups
- Formulation of the thermalization problem

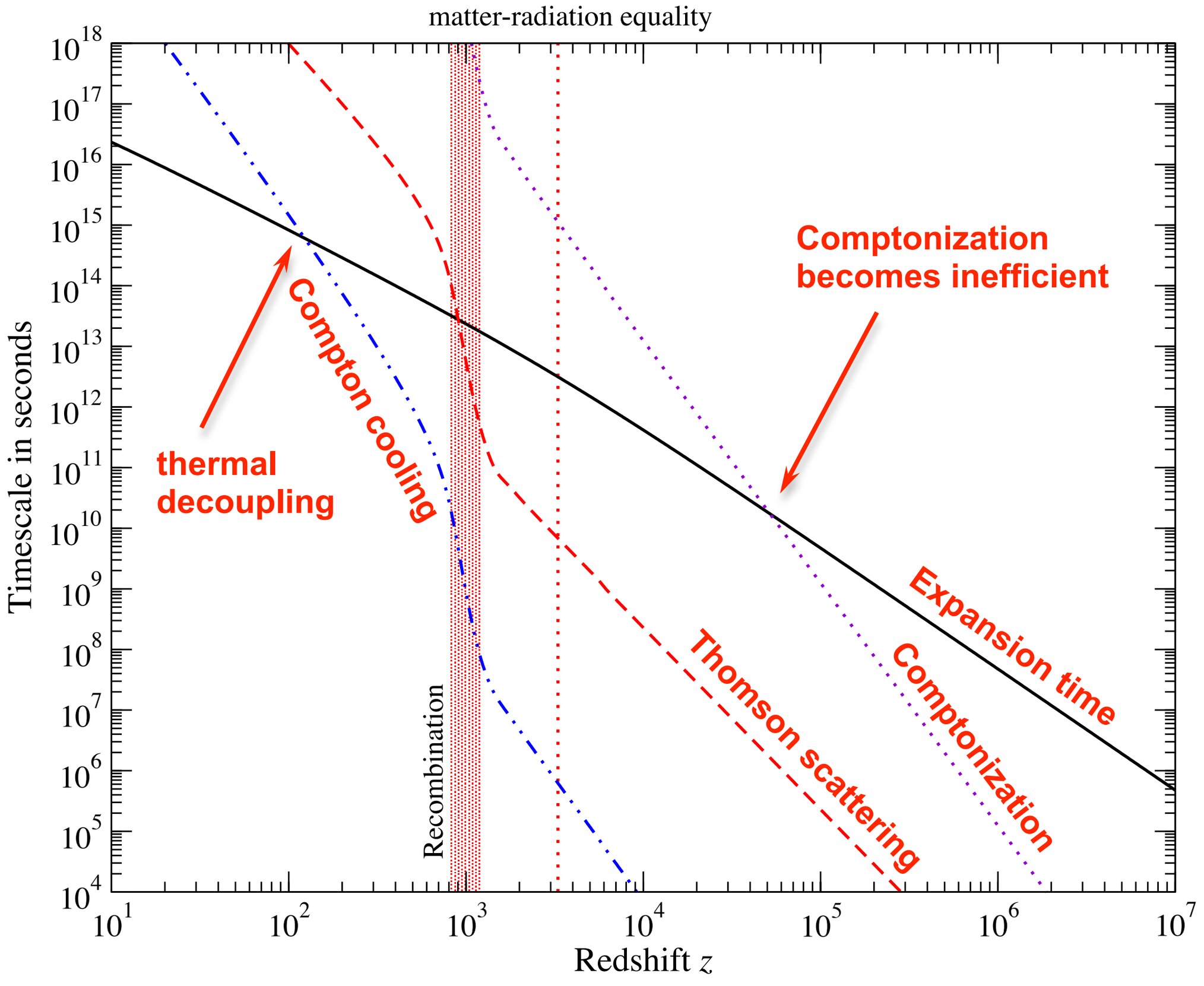

Figure 3.8: Comparison of the Comptonization and Compton cooling time-scale with the Hubble expansion time-scale.

Formulation of the thermalization problem
(double Compton process)

Enhancement of DC emission by motion of electrons

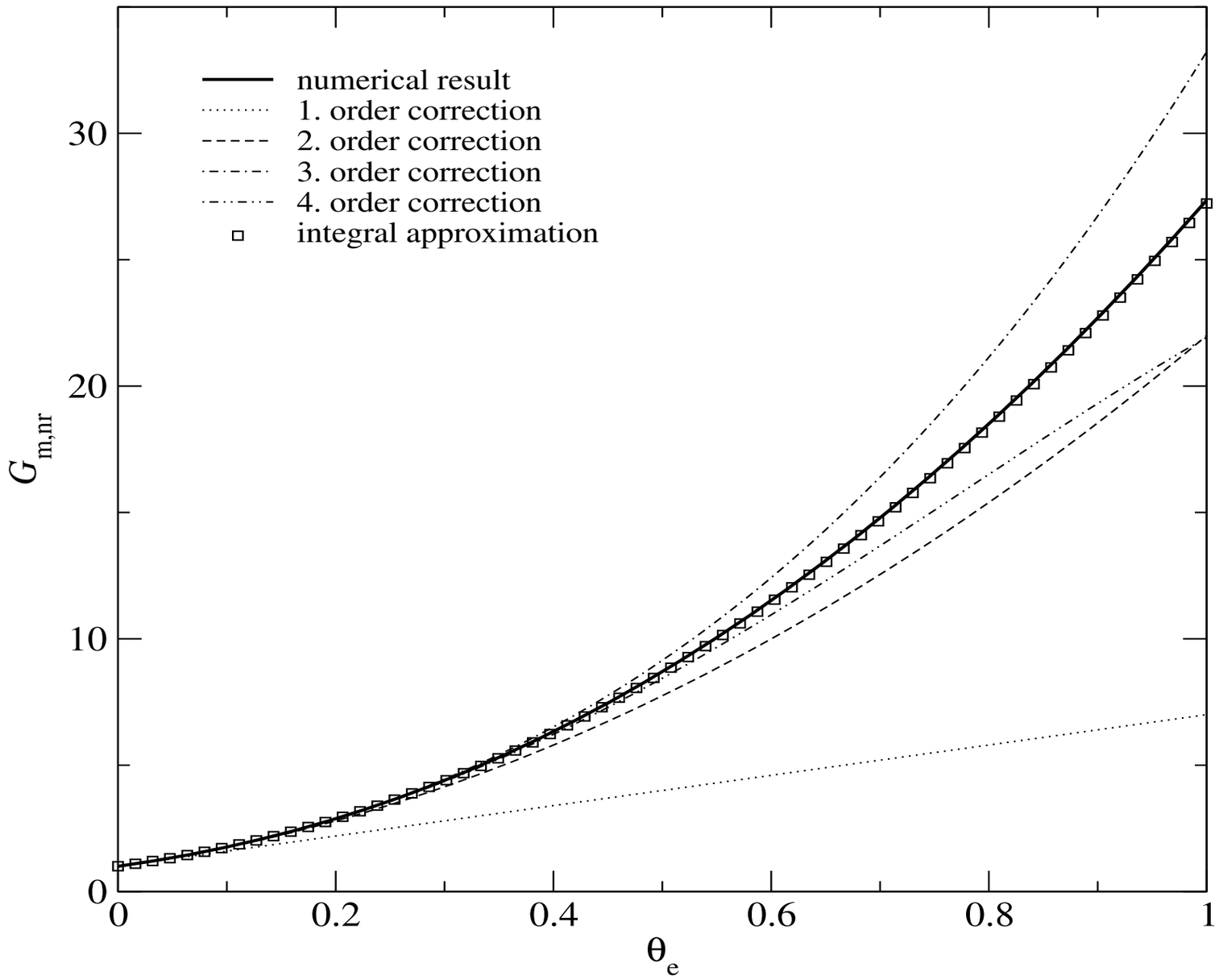

Figure 3.11: Enhancement of the DC emissivity due to thermal motions of the electrons. The approximation Eq. (3.49) works extremely well even to high temperatures. The figure is taken from Chluba et al. [10].

$$G(\theta_e) = \frac{[1+24\theta_e^2]K_0(1/\theta_e) + 8\theta_e[1+\theta_e^2]K_1(1/\theta_e)}{K_2(1/\theta_e)} \approx 1 + 6\theta_e + 15\theta_e^2 + \mathcal{O}(\theta_e^3)$$

Suppression of DC emission with photon energy

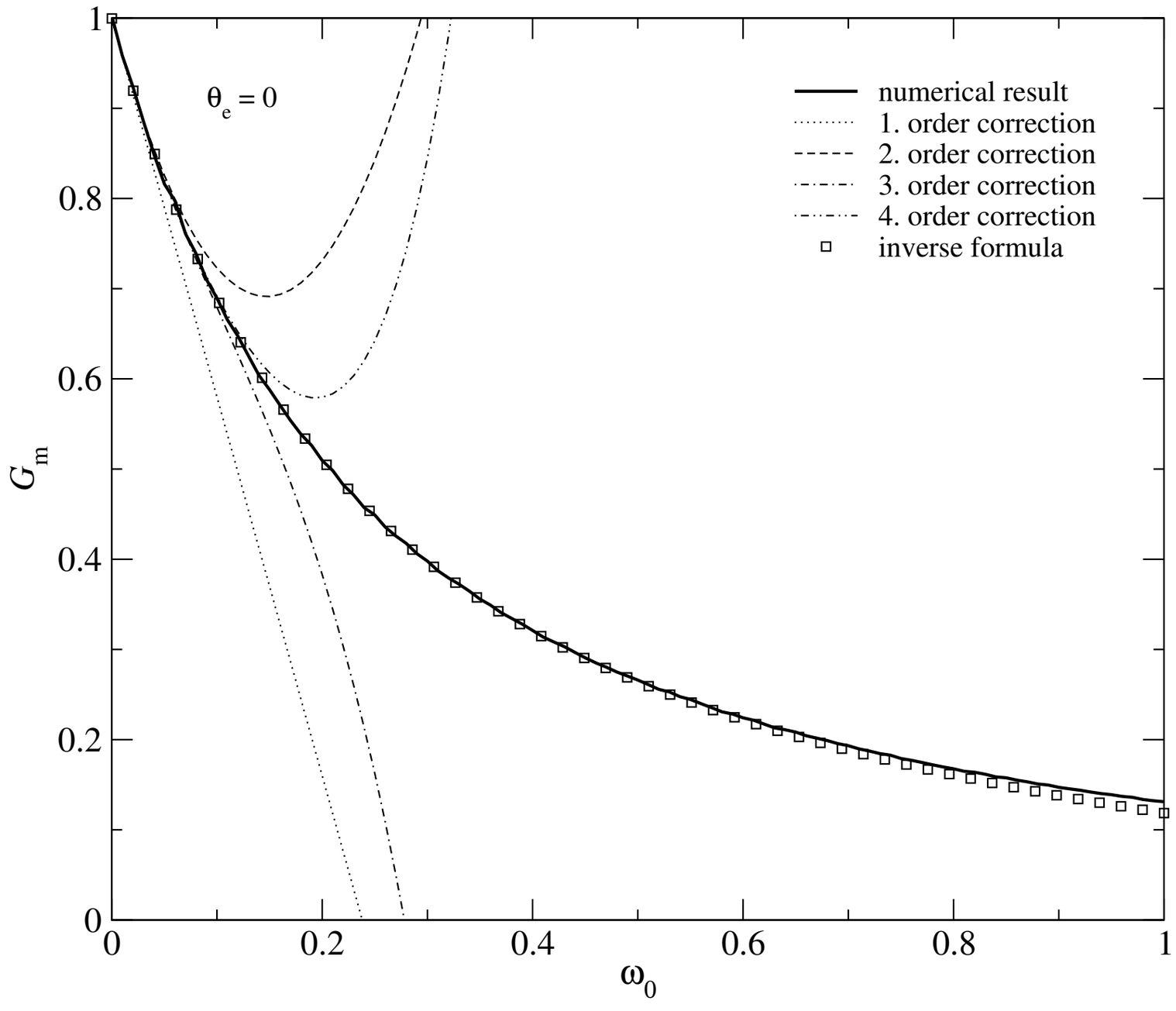

Figure 3.12: Suppression of the DC emissivity for larger incoming photon energy $\omega_0 = h\nu_0/m_e c^2$. The approximation Eq. (3.50) works extremely well even to large energies. The figure is taken from Chluba et al. [10].

$$G(\omega) = 1 - \frac{21}{5}\omega + \frac{357}{25}\omega^2 - \frac{7618}{175}\omega^3 + \frac{21498}{175}\omega^4 + \mathcal{O}(\omega^5) \approx \frac{1}{1 + \frac{21}{5}\omega + \frac{84}{25}\omega^2 - \frac{2041}{875}\omega^3 + \frac{9663}{4375}\omega^4}.$$

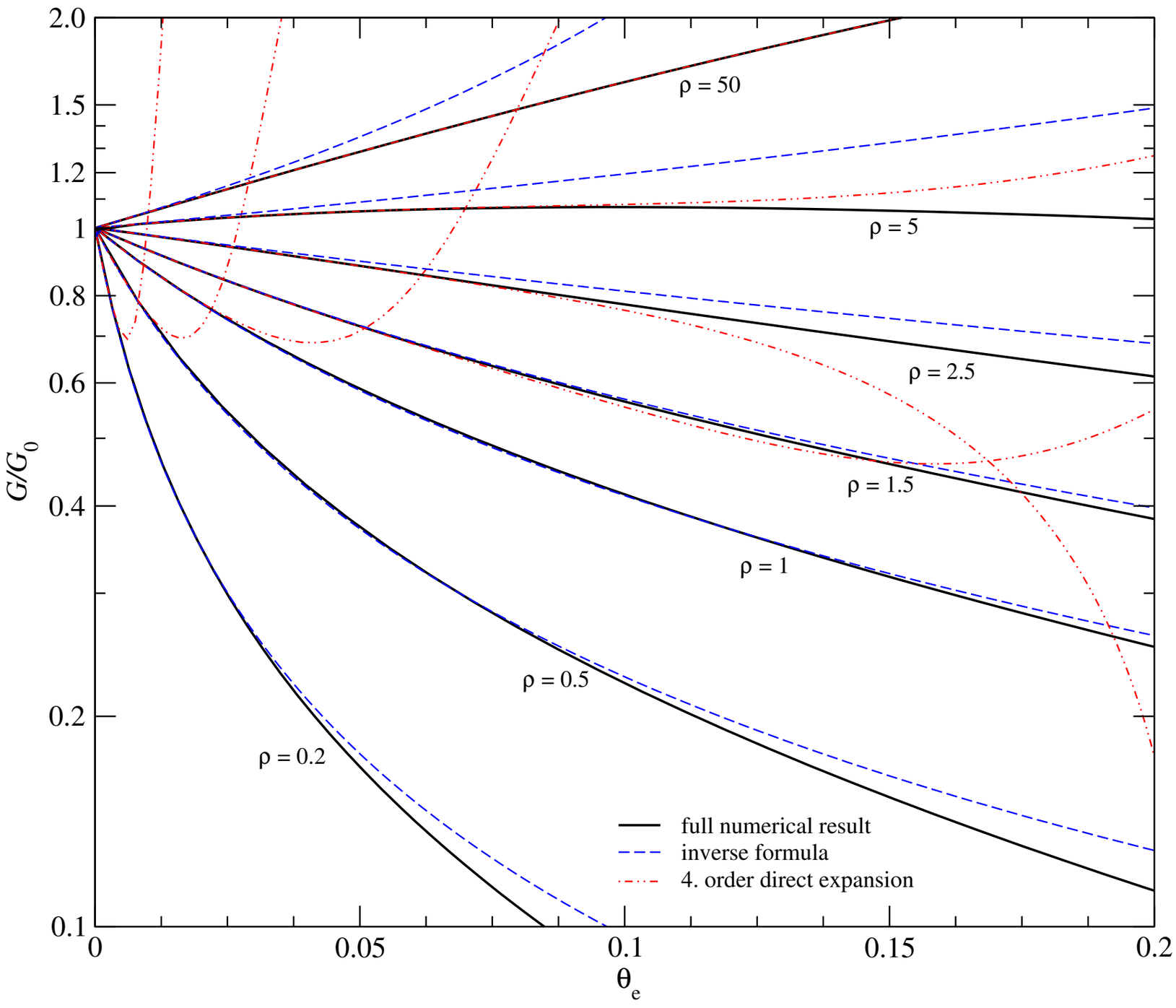

Figure 3.13: Double Compton Gaunt factor for Planckian photons at a temperature θ_γ and electrons at temperature $\theta_\mathrm{e} = \rho\,\theta_\gamma$. Approximation Eq. (3.51) represents the full numerical result extremely well, especially for $\theta_\gamma \approx \theta_\mathrm{e}$. The figure is taken from Chluba [4].

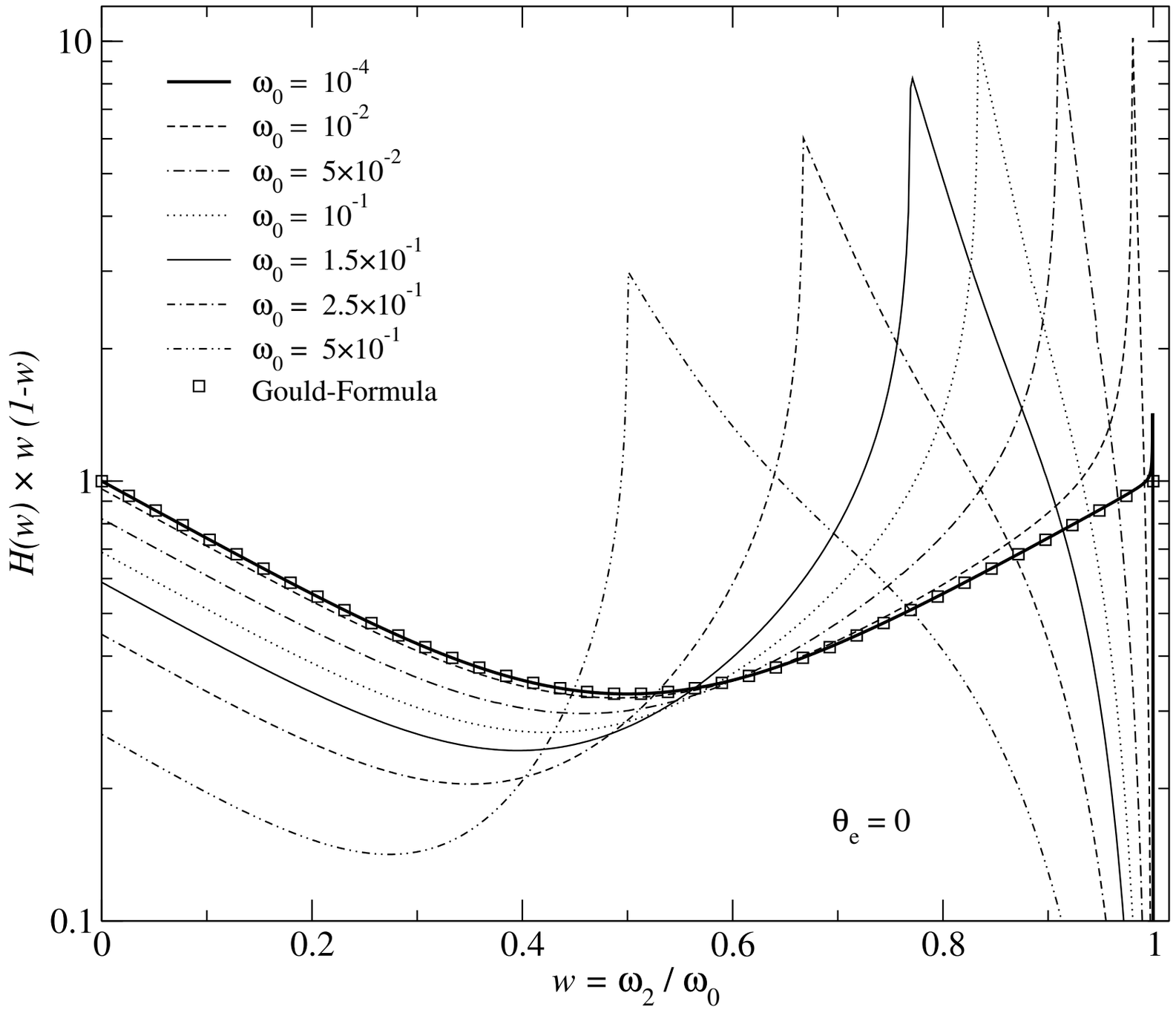

Figure 3.14: Gould factor for different incoming photon energies but $\theta_e = 0$. For larger $\omega_0 = \frac{h\nu}{m_e c^2}$, recoil corrections become important and the high frequency photon transfers energy to the electrons. The cusp is roughly at $w \simeq 1/(1+2\omega_0)$. The figure is taken from Chluba [4].

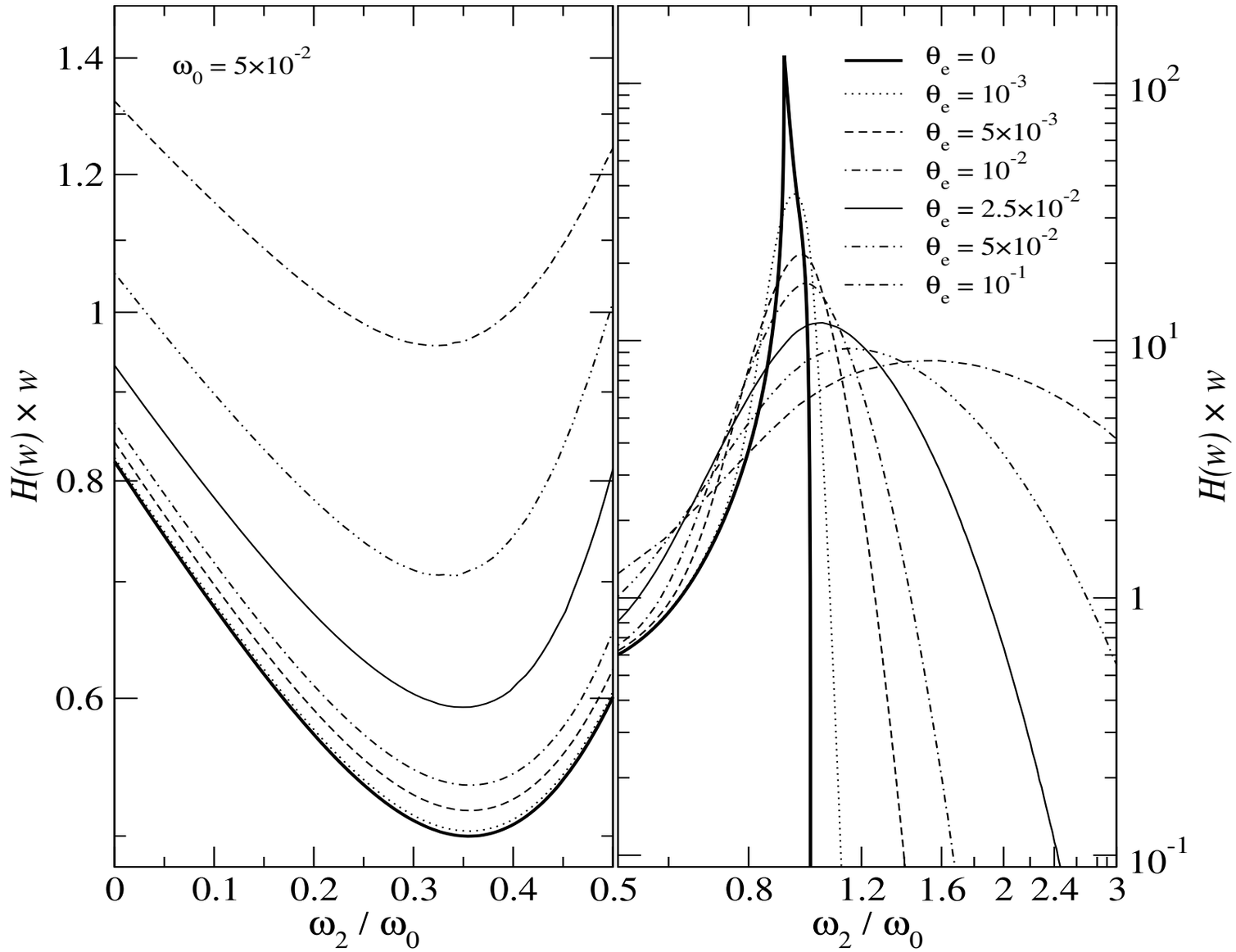

Figure 3.15: Gould factor for different different temperatures and $\omega_0 = 0.05$. For increasing θ_e, electrons transfer some energy to the high frequency photon due to Doppler boosts, leading to scattering correction to the Compton process. The figure is taken from Chluba [4].

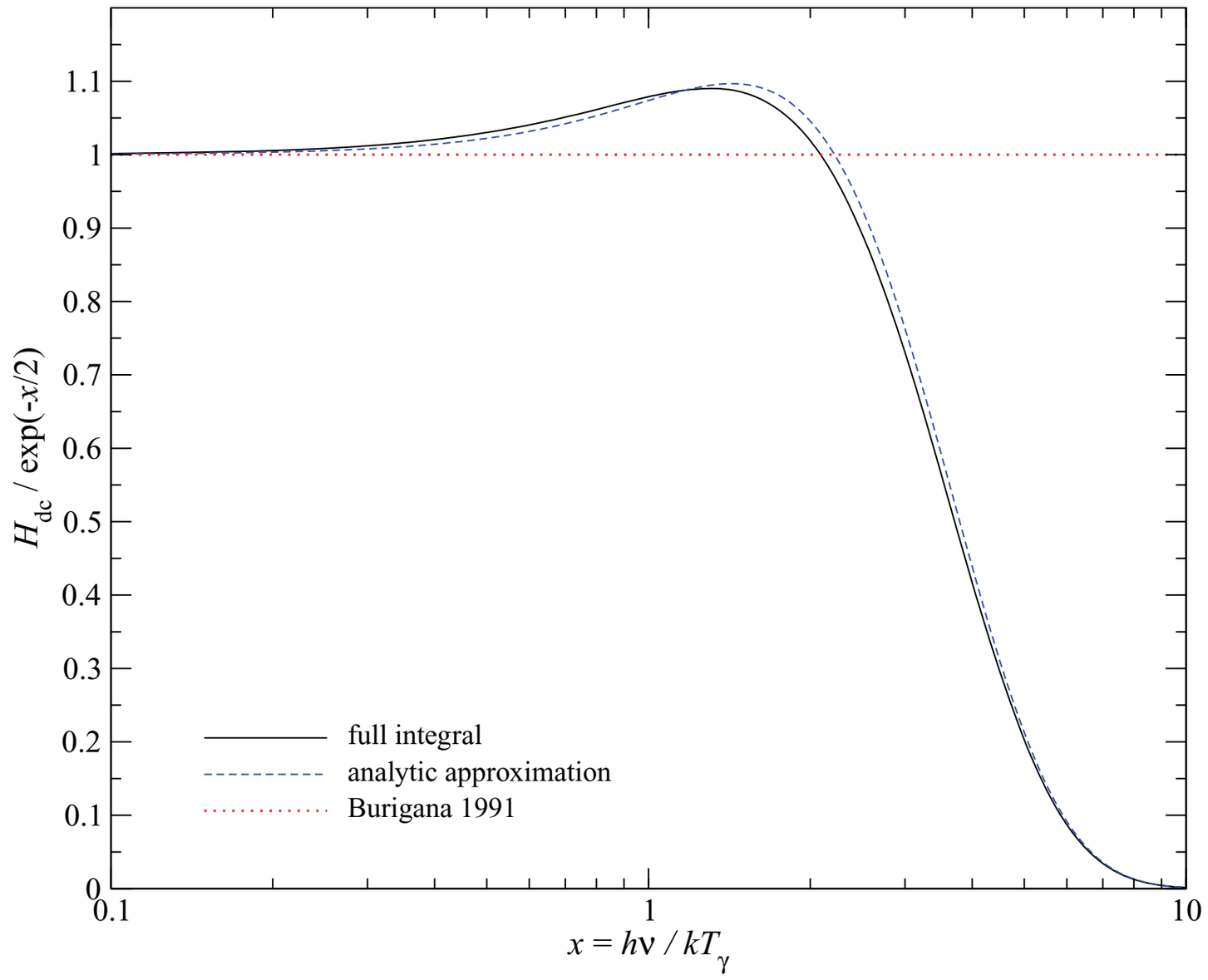

Figure 3.16: Effective double Compton correction factor $H_{\rm dc}(x)$. We compare the result from a full integration of a blackbody spectrum with the approximation given by Eq. (3.53). For comparison, we also show the approximation $H_{\rm dc}(x) \approx {\rm e}^{-x/2}$ given by Burigana et al. [1]. Close to the maximum of the CMB blackbody spectrum the differences are $\sim 20\% - 40\%$ and at high frequencies the expression of Burigana et al. [1] overestimates the DC emission significantly. The figure is taken from Chluba & Sunyaev [11].

Final Set of evolution equations

Photon field

$$\frac{\partial f}{\partial \tau} \approx \frac{\theta_{\rm e}}{x^2}\frac{\partial}{\partial x}x^4\left[\frac{\partial}{\partial x}f + \frac{T_\gamma}{T_{\rm e}}\,f(1+f)\right] + \frac{K_{\rm BR}\,{\rm e}^{-x_{\rm e}}}{x_{\rm e}^3}[1-f\,({\rm e}^{x_{\rm e}}-1)] + \frac{K_{\rm DC}\,{\rm e}^{-2x}}{x^3}[1-f\,({\rm e}^{x_{\rm e}}-1)] + S(\tau,x)$$

$$K_{\rm BR} = \frac{\alpha}{2\pi}\frac{\lambda_{\rm e}^3}{\sqrt{6\pi}\,\theta_{\rm e}^{7/2}}\sum_i Z_i^2 N_i\,\bar{g}_{\rm ff}(Z_i,T_{\rm e},T_\gamma,x_{\rm e}), \qquad K_{\rm DC} = \frac{4\alpha}{3\pi}\,\theta_\gamma^2\,I_{\rm dc}\,g_{\rm dc}(T_{\rm e},T_\gamma,x)$$

$$\bar{g}_{\rm ff}(x_{\rm e}) \approx \begin{cases} \frac{\sqrt{3}}{\pi}\ln\left(\frac{2.25}{x_{\rm e}}\right) & \text{for} \quad x_{\rm e} \le 0.37 \\ 1 & \text{otherwise} \end{cases}, \qquad g_{\rm dc} \approx \frac{1+\frac{3}{2}x+\frac{29}{24}x^2+\frac{11}{16}x^3+\frac{5}{12}x^4}{1+19.739\theta_\gamma-5.5797\theta_{\rm e}}.$$

$$I_{\rm dc} = \int x^4 f(1+f)\,{\rm d}x \approx 4\pi^4/15$$

Ordinary matter temperature

$$\frac{{\rm d}\rho_{\rm e}}{{\rm d}\tau} = \frac{{\rm d}(T_{\rm e}/T_\gamma)}{{\rm d}\tau} = \frac{t_{\rm T}\dot{Q}}{\alpha_{\rm h}\theta_\gamma} + \frac{4\tilde{\rho}_\gamma}{\alpha_{\rm h}}[\rho_{\rm e}^{\rm eq}-\rho_{\rm e}] - \frac{4\tilde{\rho}_\gamma}{\alpha_{\rm h}}\mathcal{H}_{\rm DC,BR}(\rho_{\rm e}) - H\,t_{\rm T}\,\rho_{\rm e}.$$

$$k\alpha_{\rm h} = \frac{3}{2}k[N_{\rm e}+N_{\rm H}+N_{\rm He}] = \frac{3}{2}kN_{\rm H}[1+f_{\rm He}+X_{\rm e}] \qquad \rho_{\rm e}^{\rm eq} = T_{\rm e}^{\rm eq}/T_\gamma$$

$$\tilde{\rho}_\gamma = \rho_\gamma/m_{\rm e}c^2 \qquad T_{\rm e}^{\rm eq} = T_\gamma\frac{\int x^4 f(1+f)\,{\rm d}x}{4\int x^3 f\,{\rm d}x} \equiv \frac{h}{k}\frac{\int \nu^4 f(1+f)\,{\rm d}\nu}{4\int \nu^3 f\,{\rm d}\nu}$$

Structure of the Lectures *(at least in theory)*

Lecture I:

- Overview and motivation
- Simple blackbody radiation warm-ups
- Formulation of the thermalization problem

Structure of the Lectures *(at least in theory)*

Lecture I:

- Overview and motivation
- Simple blackbody radiation warm-ups
- Formulation of the thermalization problem

Lecture II:

- Analytic description of the distortions
- Distortion visibility function
- Fast computation of the distortions

Analytic solutions and definition of μ and y

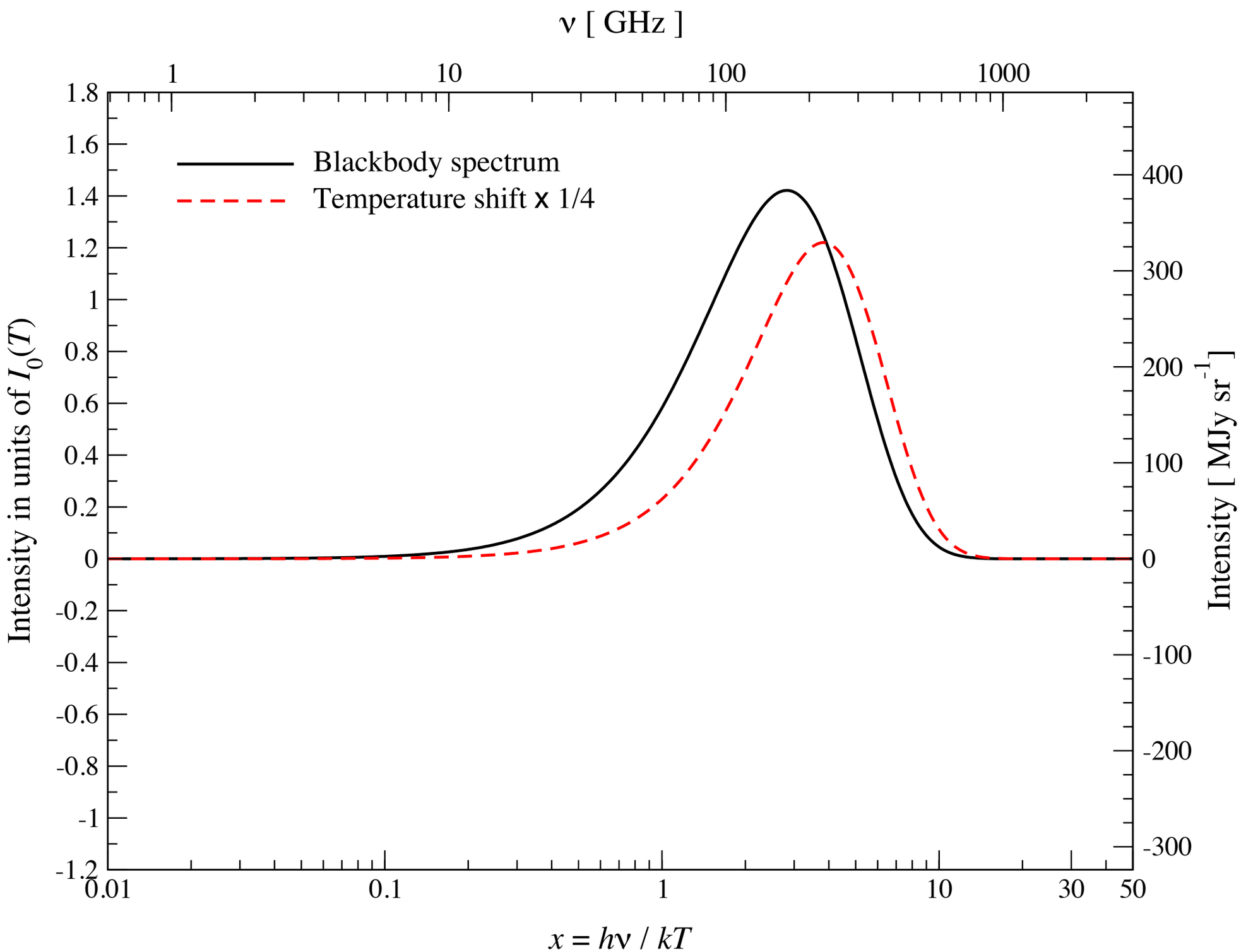
ν [GHz]
1
10
100
1000
Blackbody spectrum
Temperature shift x 1/4
Intensity in units of $I_0(T)$
Intensity [MJy sr^{-1}]
1.8
1.6
1.4
1.2
1
0.8
0.6
0.4
0.2
0
-0.2
-0.4
-0.6
-0.8
-1
-1.2
400
300
200
100
0
-100
-200
-300
0.01
0.1
1
10
30
50
$x = h\nu / kT$

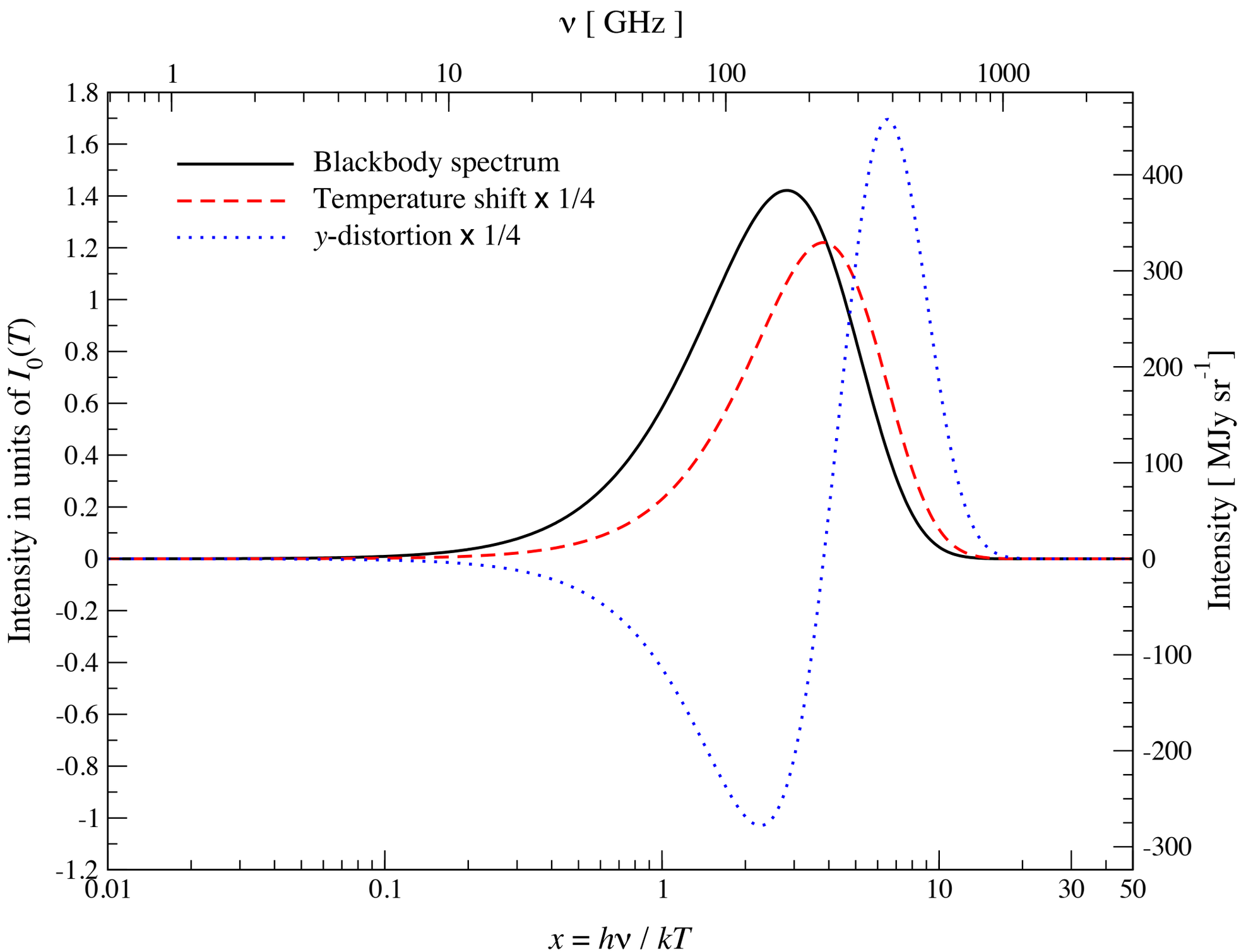
ν [GHz]
1
10
100
1000
Blackbody spectrum
Temperature shift x 1/4
y-distortion x 1/4
Intensity in units of $I_0(T)$
Intensity [MJy sr^{-1}]
1.8
1.6
1.4
1.2
1
0.8
0.6
0.4
0.2
0
-0.2
-0.4
-0.6
-0.8
-1
-1.2
400
300
200
100
0
-100
-200
-300
0.01
0.1
1
10
30
50
$x = h\nu / kT$

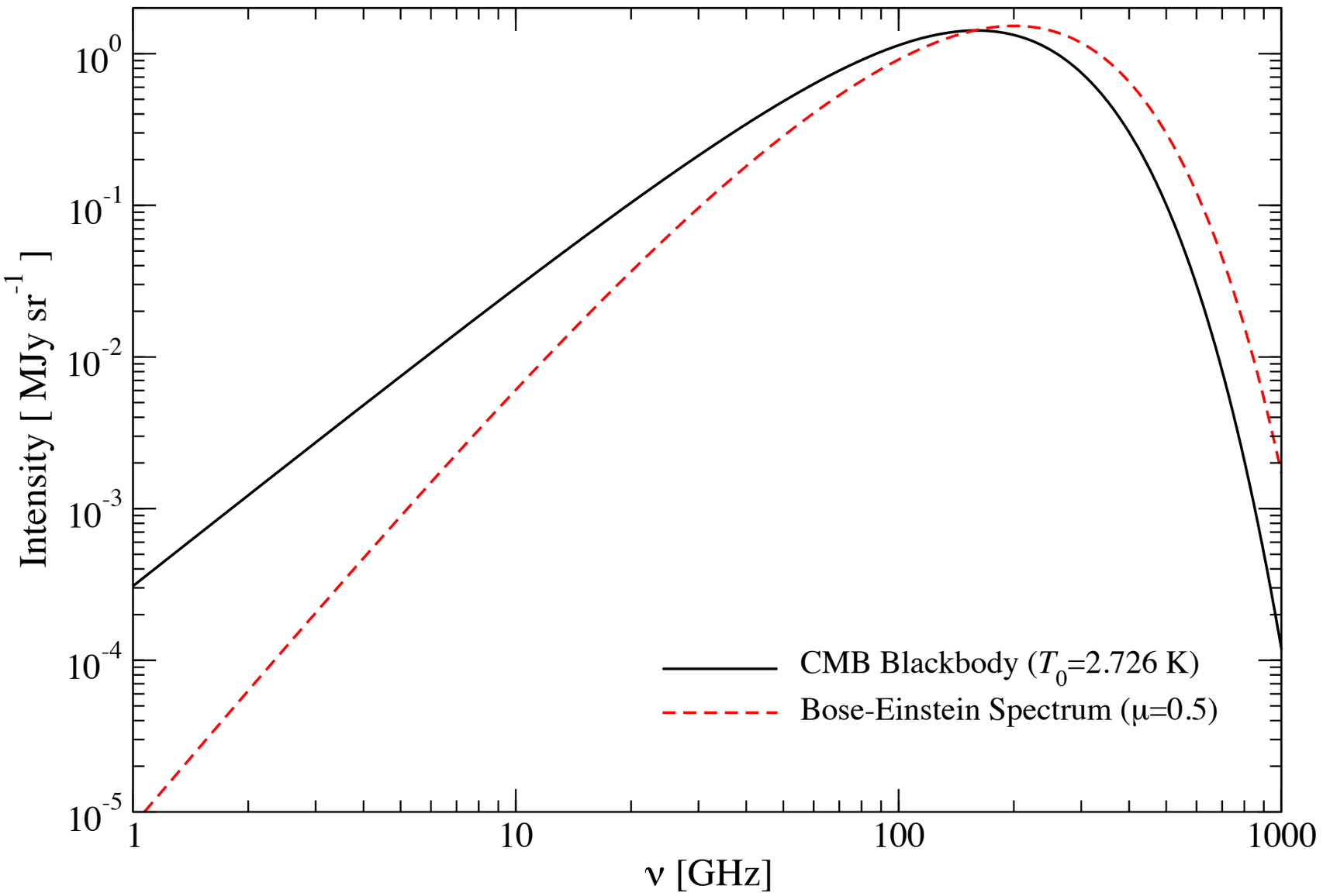

Figure 4.2: Bose-Einstein spectrum for large chemical potential $\mu = 0.5$ and $T_i = T_0 = 2.726\,\mathrm{K}$. Only energy was added to the photon field, but the number of photons was not changed with respect to the initial CMB spectrum. For large chemical potential, the cross over frequency shifts towards higher frequencies according to $\nu_{\mathrm{cr}} \approx 124\,\mathrm{GHz}\,(1 - 0.304\,\mu \ln \mu) \approx 158\,\mathrm{GHz}$. The figure was taken from Chluba [10].

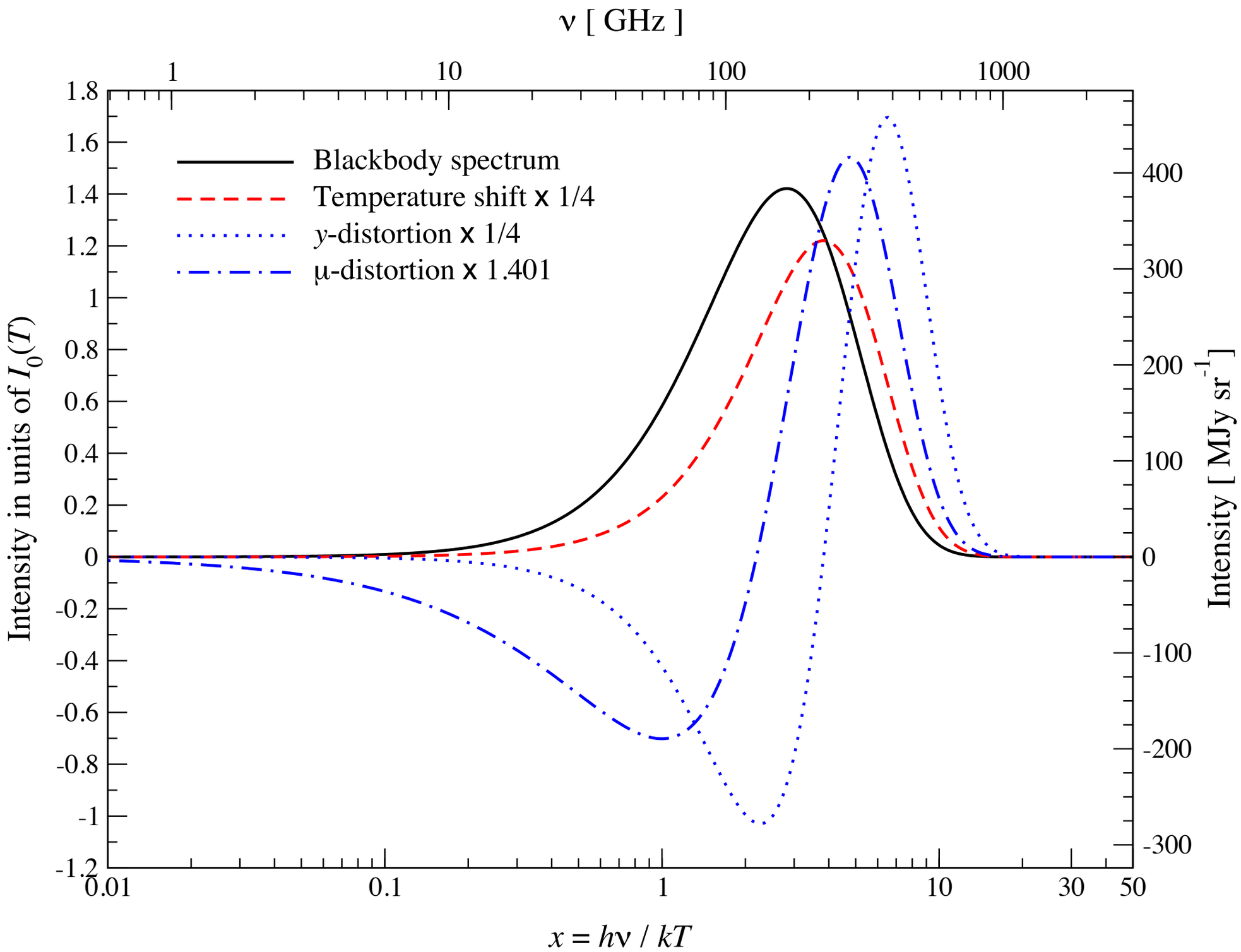
ν [GHz]
1
10
100
1000
Blackbody spectrum
Temperature shift x 1/4
y-distortion x 1/4
μ-distortion x 1.401
Intensity in units of $I_0(T)$
Intensity [MJy sr^{-1}]
1.8
1.6
1.4
1.2
1
0.8
0.6
0.4
0.2
0
-0.2
-0.4
-0.6
-0.8
-1
-1.2
400
300
200
100
0
-100
-200
-300
0.01
0.1
1
10
30
50
$x = h\nu / kT$

y - distortion

μ–*y* transition

μ - distortion

Last Scattering Surface

10^2 10^3 10^4 10^5 10^6 10^7

redshift *z*

y - distortion

μ–*y* transition

μ - distortion

Last Scattering Surface

CMB anisotropies

10^2 10^3 10^4 10^5 10^6 10^7

redshift z

y - distortion

μ–*y* transition

μ - distortion

Last Scattering Surface

CMB anisotropies

$t_{\rm K} \simeq t_{\rm exp}$

10^2 10^3 10^4 10^5 10^6 10^7

redshift z

y - distortion

μ–*y* transition

μ - distortion

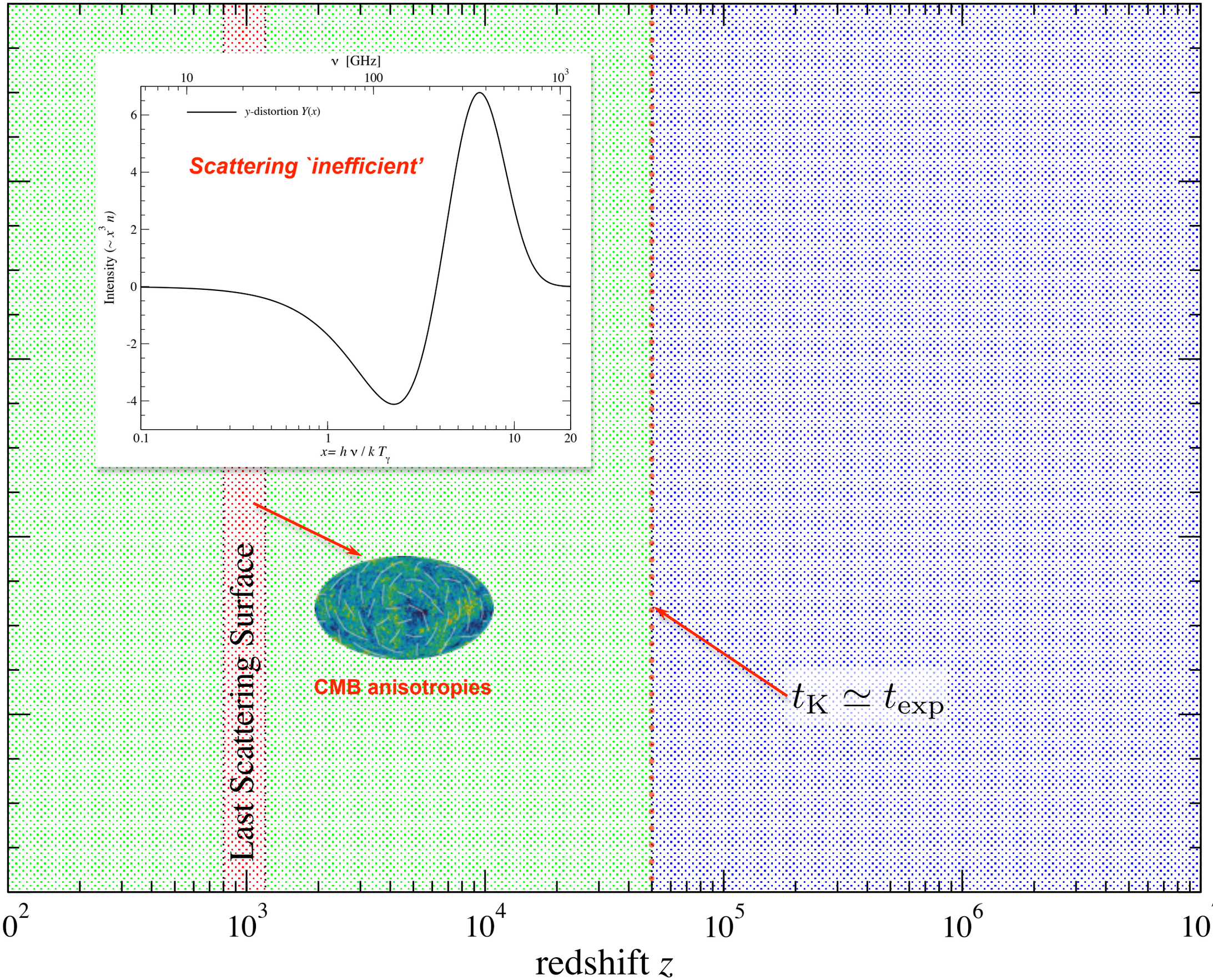

y - distortion

μ–*y* transition

μ - distortion

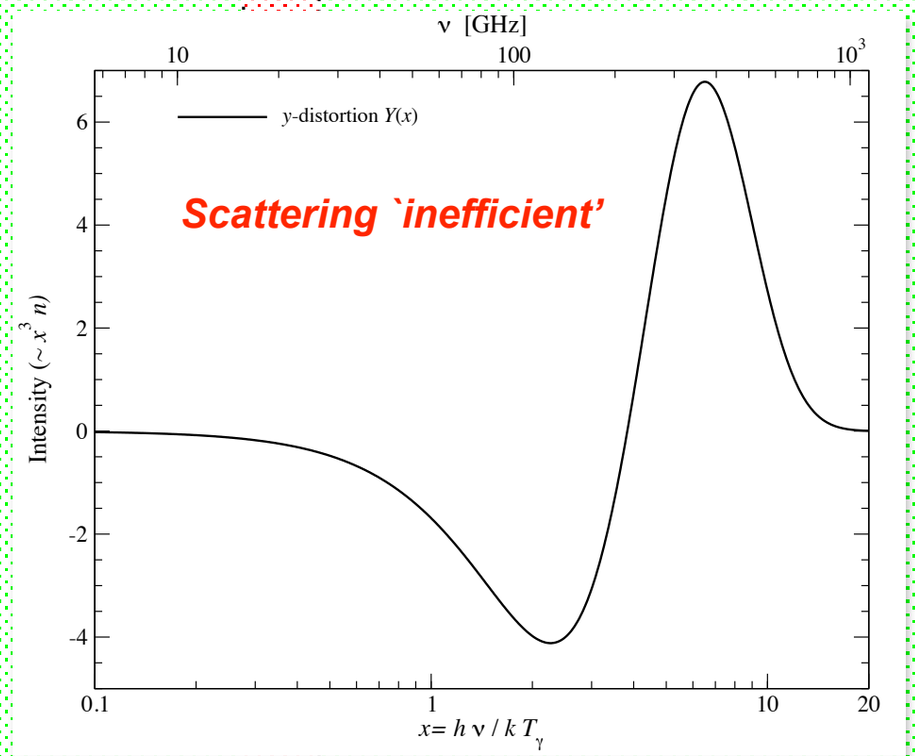

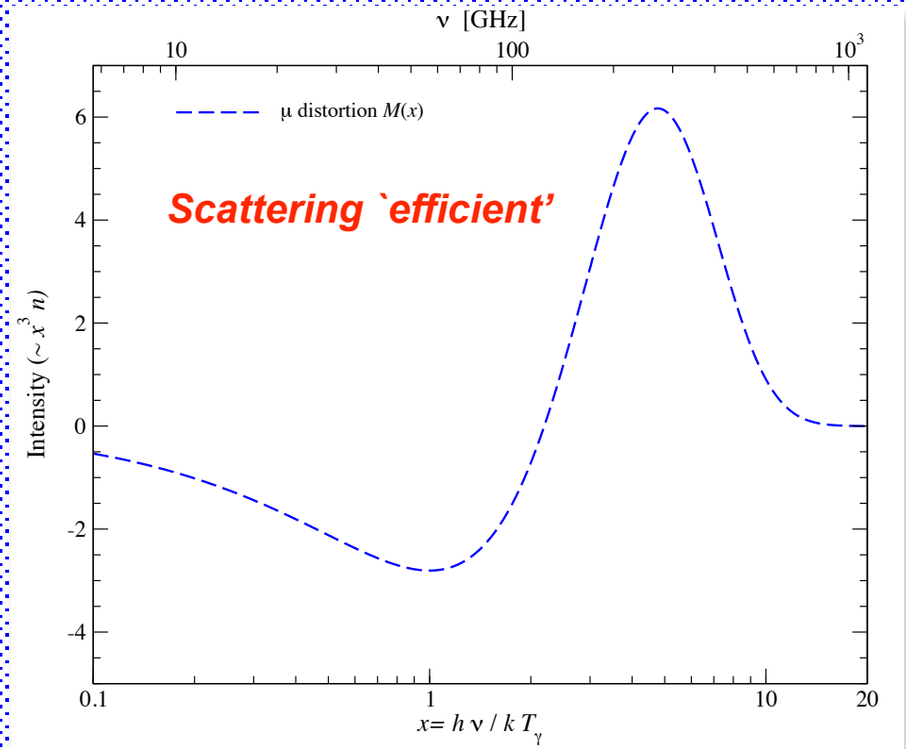

CMB anisotropies

Last Scattering Surface

$t_{\rm K} \simeq t_{\rm exp}$

10^2 10^3 10^4 10^5 10^6 10^7

redshift *z*

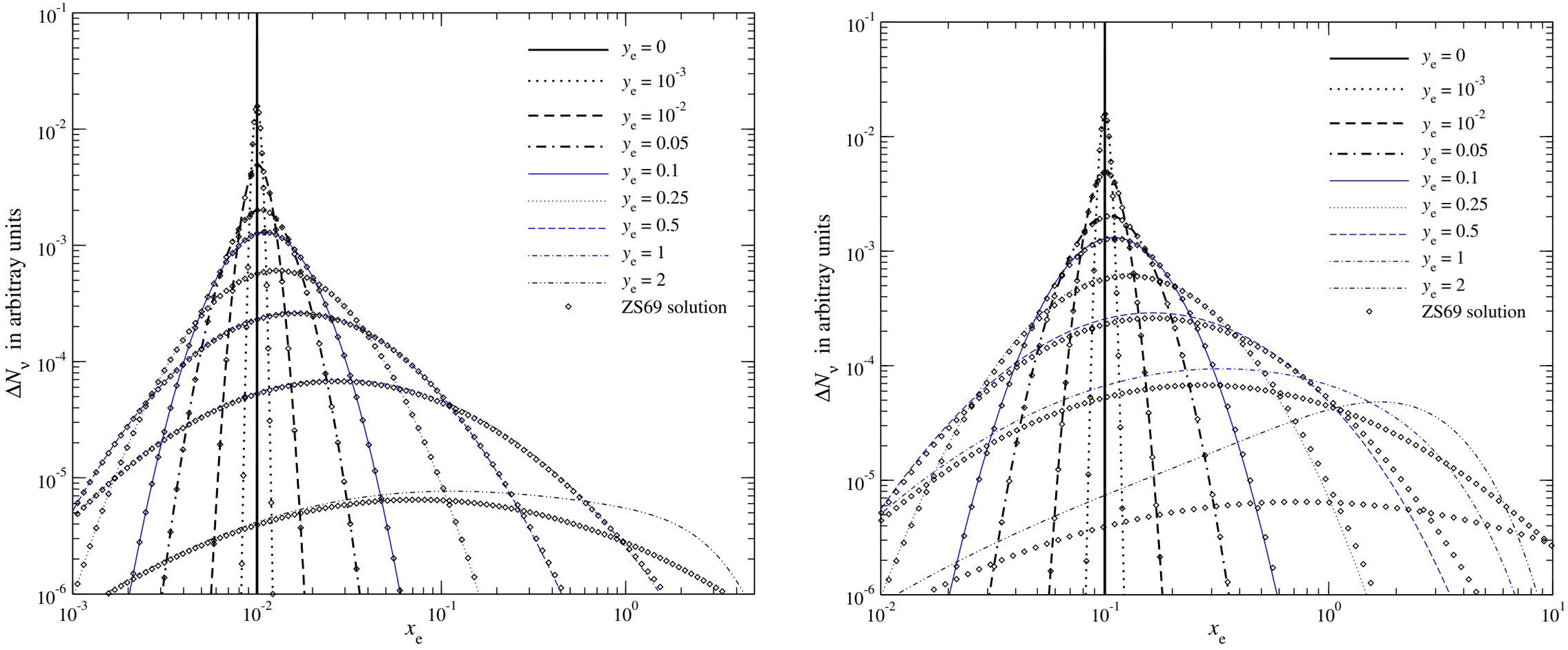

Figure 4.4: Time-evolution of $\Delta N_\nu = \nu^2 \Delta n$ for different values of the y-parameter but neglecting stimulated scattering. The left panel shows the case, for an initially narrow line which was injected at $x_{e,0} = 10^{-2}$, while the right panel shows the solution for injection at $x_{e,0} = 10^{-1}$. In both figures, we present the results as obtained by numerically solving the Kompaneets equation. In addition, we give the analytic solution according to Zeldovich & Sunyaev [59], Eq. (4.18). The figure is taken from Chluba & Sunyaev [15].

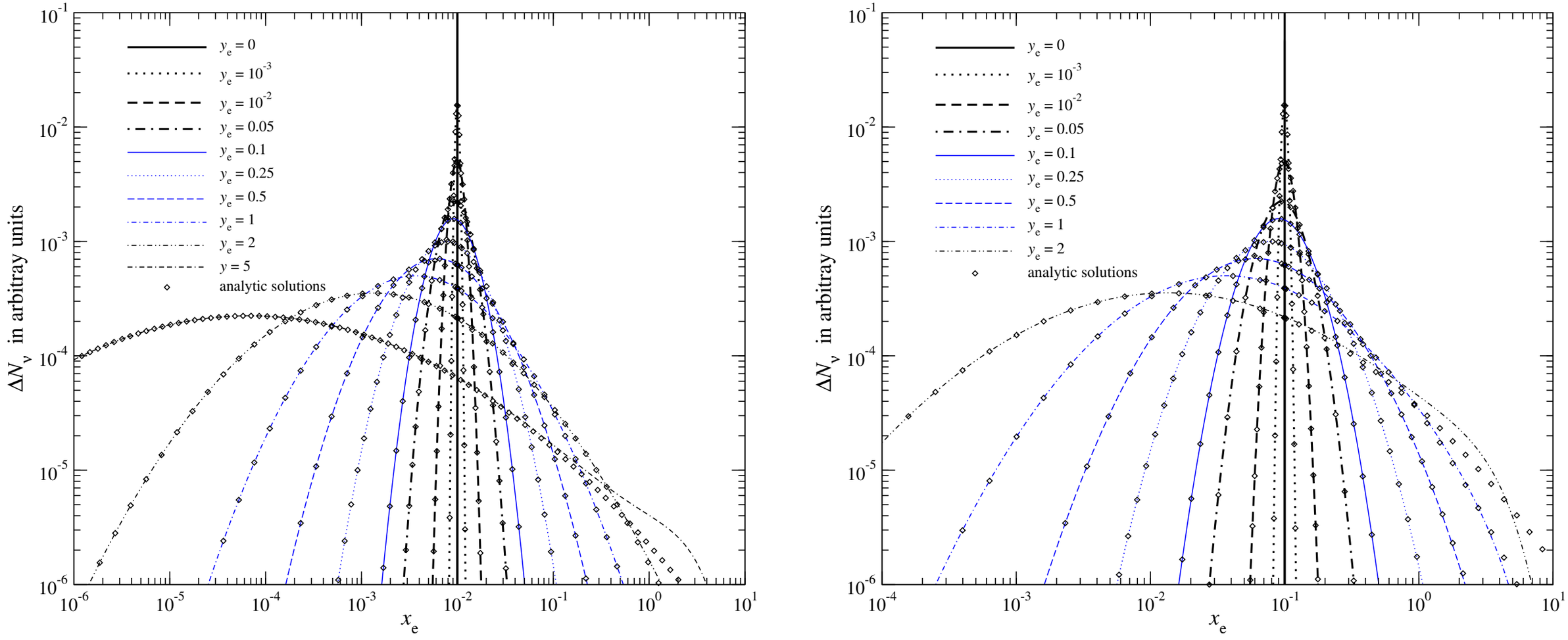

Figure 4.5: Time-evolution of $\Delta N_\nu = \nu^2 \Delta n$ for different values of the y-parameter *including* the effect of stimulated scattering in the blackbody ambient radiation field. The left panel shows the case, for an initially narrow line which was injected at frequency $x_{e,0} = 10^{-2}$, while the right panel shows the solution for injection at $x_{e,0} = 10^{-1}$. In both figures we show the results as obtained by numerically solving Kompaneets equation with $T_\gamma = T_e$. In addition, we give the analytic solutions of the linearized problem, Eq. (4.25), according to Eq. (4.26). The figure is taken from Chluba & Sunyaev [15].

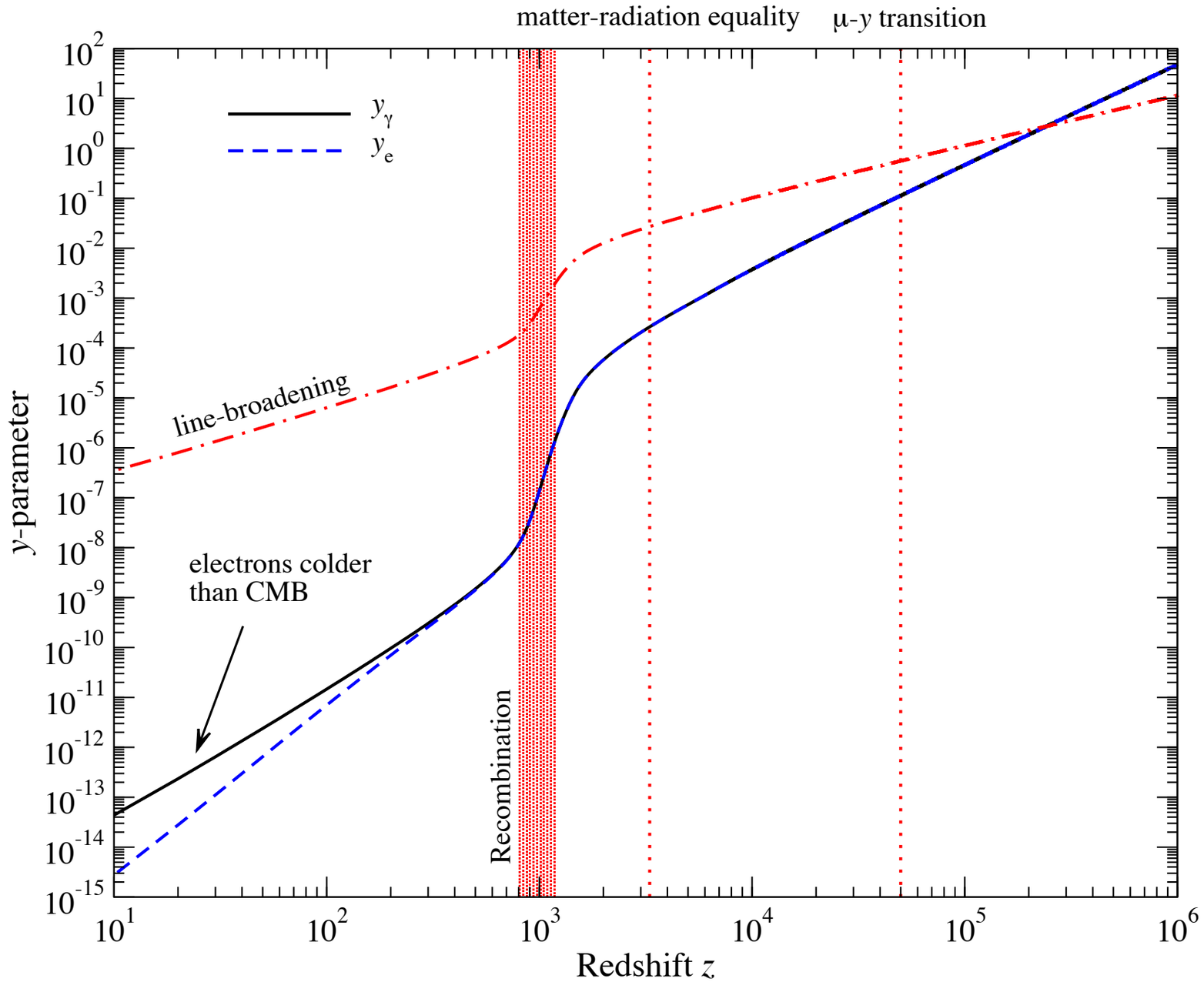

Figure 4.6: Dependence of the y-parameters, y_γ and y_e, on redshift. After recombination the y-parameters drop strongly since the number of free electrons decreases exponentially. At late times, electrons drop out of equilibrium with the photons so that $y_e < y_\gamma$. Around $z_K = 5 \times 10^4$, we have $y_e \simeq y_\gamma \simeq 0.1$. The line-broadening, $\Delta\nu/\nu \simeq 2\sqrt{y_\gamma \ln 2}$, is also illustrated. After recombination it becomes much smaller than $\Delta\nu/\nu \simeq 10^{-3}$.

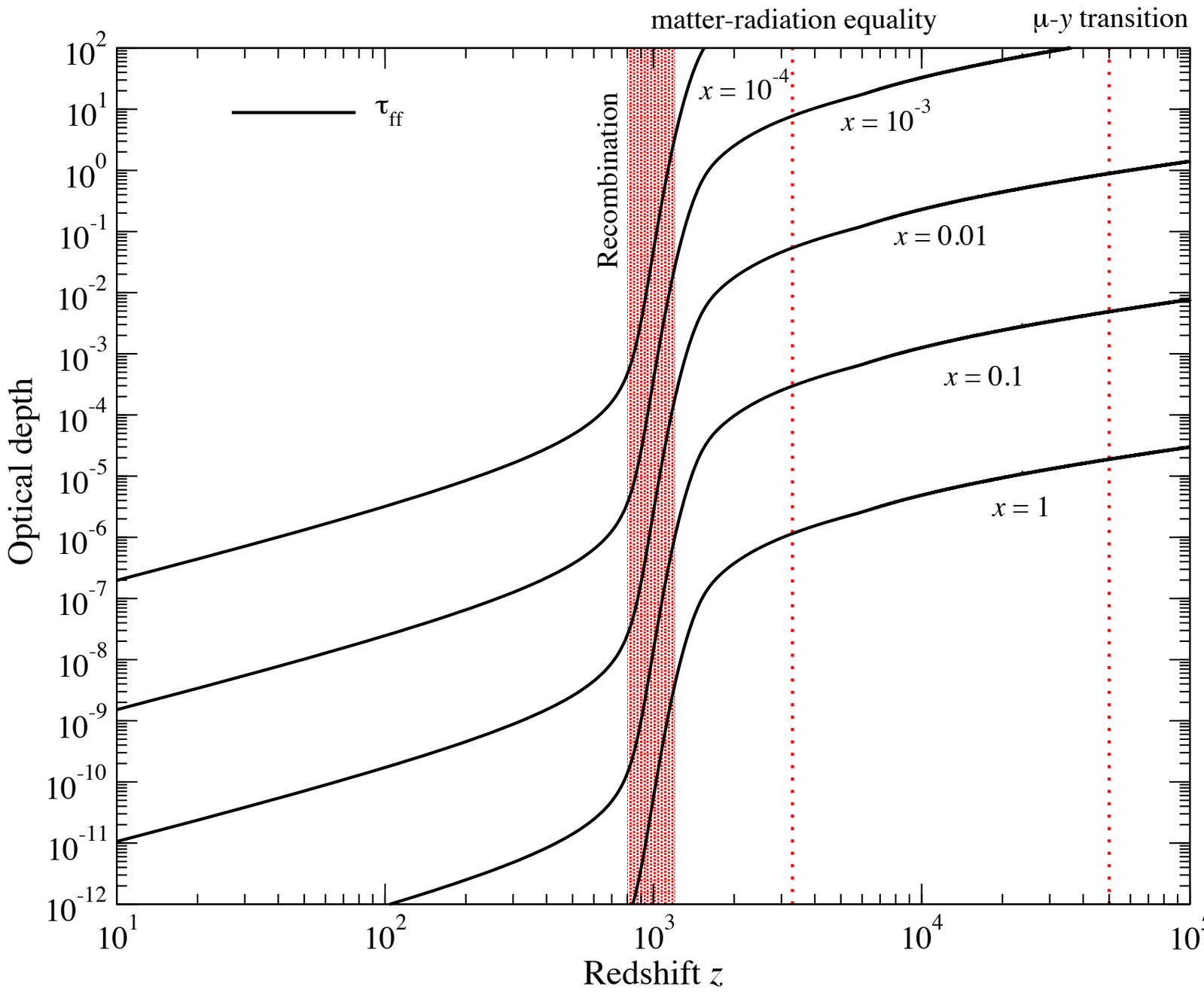

Figure 4.7: Absorption optical depth for BR at different redshifts and frequencies x. At low frequencies, the rough scaling is $\tau_{\rm ff} \simeq x^{-2}$. For $x \simeq 10^{-4}$, the Universe becomes transparent ($\tau_{\rm ff} \simeq 1$) around recombination. For $x \simeq 10^{-3}$ this transition happens around $z \simeq 1700$ and for $x \simeq 0.01$ it is $z \simeq 10^5$.

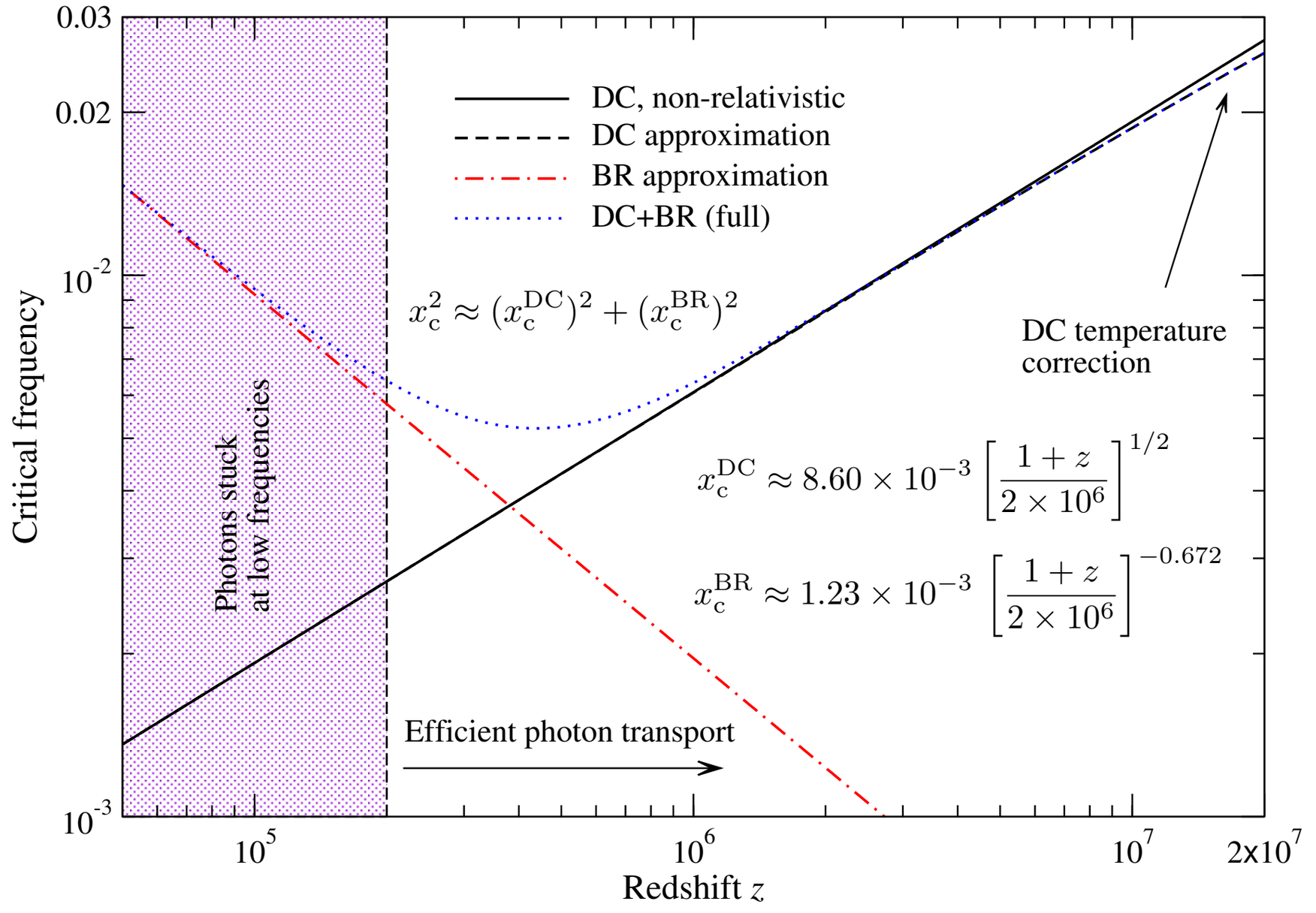

Figure 4.8: Critical frequency, x_c as a function of z. Photon transport is inefficient below $z \simeq 2 \times 10^5$ so that the distortion visibility function quickly approaches unity. DC temperature corrections become noticeable at $z \gtrsim 10^6$. The approximations are from Eq. (4.38) and (4.39). The figure is taken from Chluba [10].

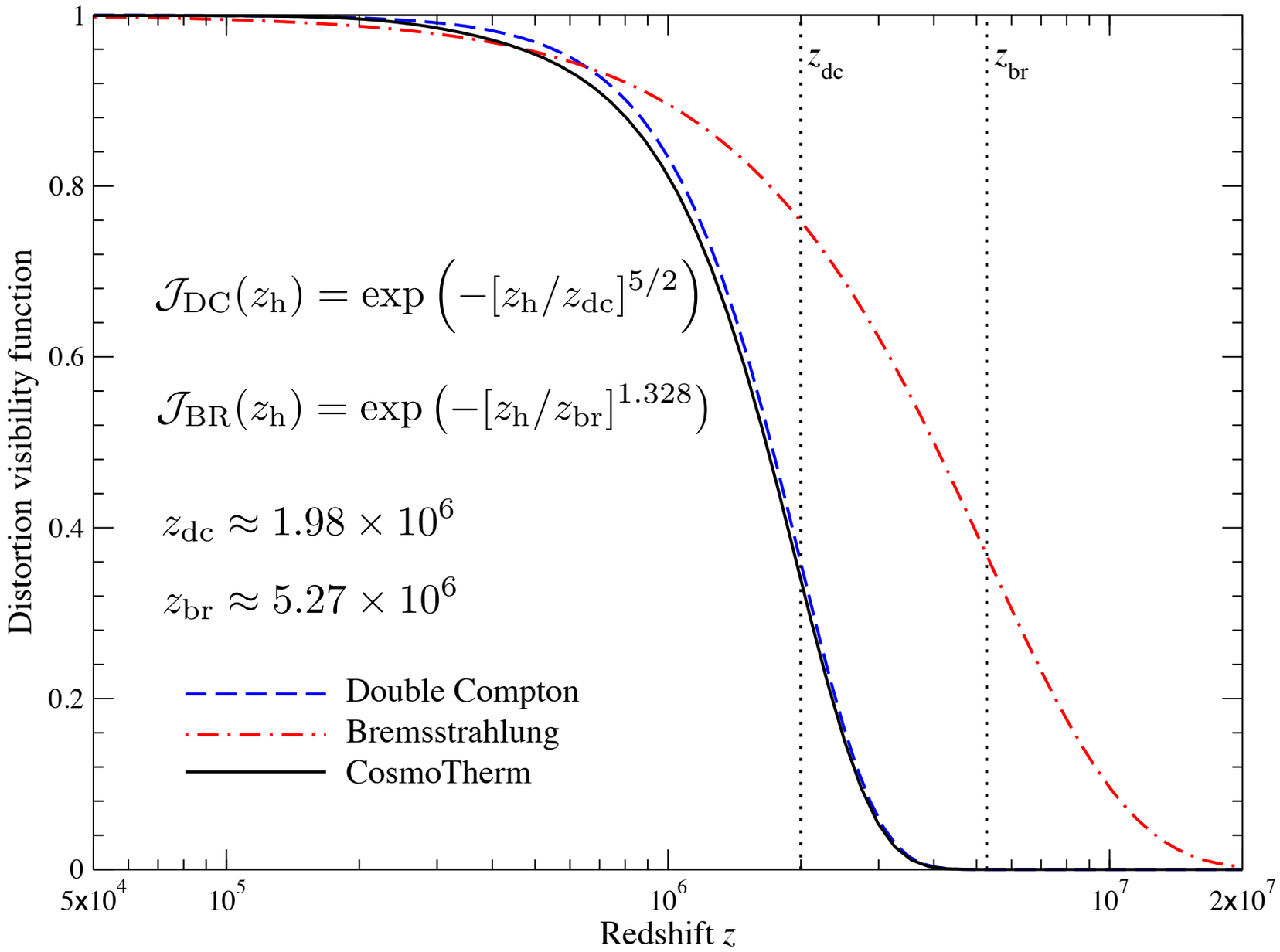

Figure 4.9: Distortion visibility function. We compare $\mathcal{J}_{\rm DC}(z_{\rm h})$, $\mathcal{J}_{\rm BR}(z_{\rm h})$ and the numerical result obtained with CosmoTherm. DC emission significantly change the thermalization efficiency. Deviations from the numerical result can be captured by adding several effects, as discussed in Sect. 4.6.

Improved picture for the formation of distortions

y - distortion

μ–*y* transition

μ - distortion

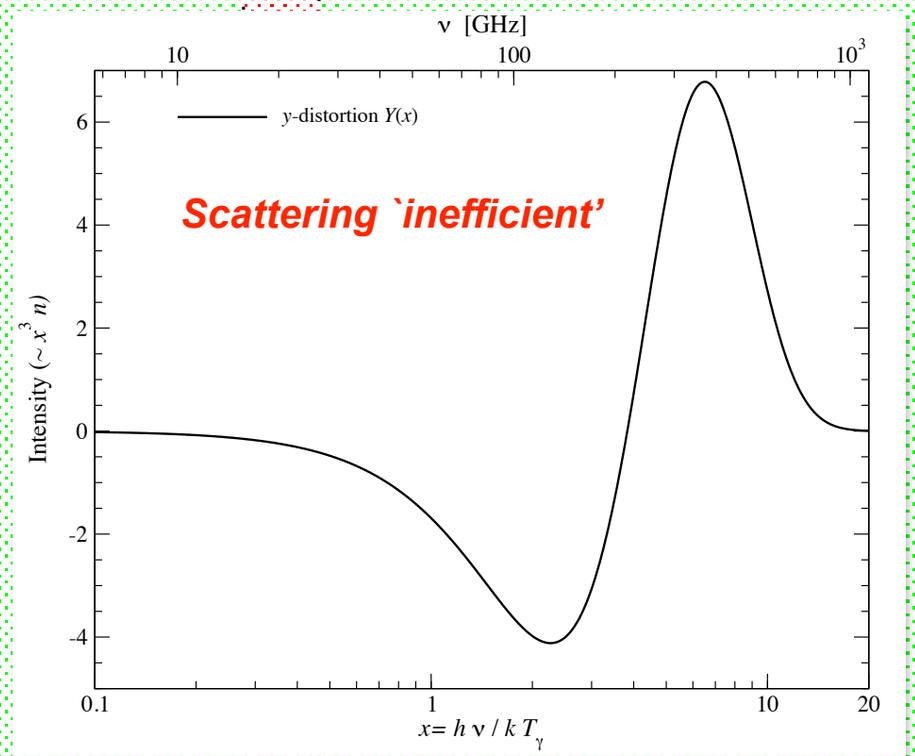

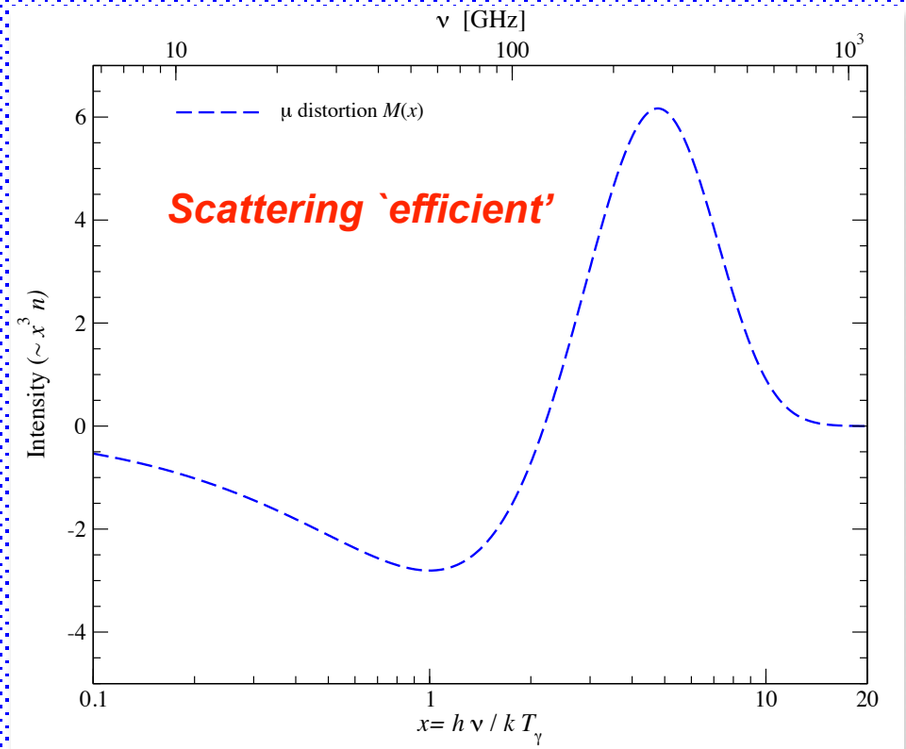

CMB anisotropies

Last Scattering Surface

$t_{\rm K} \simeq t_{\rm exp}$

10^2 10^3 10^4 10^5 10^6 10^7

redshift *z*

y - distortion

μ–*y* transition

μ - distortion

Distortion visibility:

Visibility

1

0.8

0.6

0.4

0.2

0

Last Scattering Surface

$t_{\rm K} \simeq t_{\rm exp}$

10^2 10^3 10^4 10^5 10^6 10^7

redshift z

y - distortion

μ–*y* transition

μ - distortion

Distortion visibility:

How much of the released energy appears as spectral distortion?

Visibility

1

0.8

0.6

0.4

0.2

0

Last Scattering Surface

$t_{\rm K} \simeq t_{\rm exp}$

10^2 10^3 10^4 10^5 10^6 10^7

redshift z

y - distortion

μ–y transition

μ - distortion

Distortion visibility:

How much of the released energy appears as spectral distortion?

At this point it is 100% at all time!!!

We also need to include photon production to have thermalization!

Visibility

1

0.8

0.6

0.4

0.2

0

Last Scattering Surface

$t_{\rm K} \simeq t_{\rm exp}$

10^2

10^3

10^4

10^5

10^6

10^7

redshift z

y - distortion

μ–y transition

μ - distortion

$$y \simeq \frac{1}{4}\frac{\Delta\rho_\gamma}{\rho_\gamma} \equiv \frac{1}{4}\int_0^{z_{\rm K}} \frac{{\rm d}(Q/\rho_\gamma)}{{\rm d}z'}\,{\rm d}z'$$

Visibility

1

0.8

0.6

0.4

0.2

0

Last Scattering Surface

$t_{\rm K} \simeq t_{\rm exp}$

10^2 10^3 10^4 10^5 10^6 10^7

redshift z

y - distortion

μ–*y* transition

μ - distortion

$$y \simeq \frac{1}{4}\frac{\Delta\rho_\gamma}{\rho_\gamma} \equiv \frac{1}{4}\int_0^{z_{\rm K}} \frac{{\rm d}(Q/\rho_\gamma)}{{\rm d}z'}\,{\rm d}z'$$

$$\mu \approx 1.4\int_{z_{\rm K}}^{\infty} \frac{{\rm d}(Q/\rho_\gamma)}{{\rm d}z'}\mathcal{J}_\mu(z'){\rm d}z'$$

$$\mathcal{J}_\mu(z) \approx {\rm e}^{-\left(\frac{z}{2\times10^6}\right)^{5/2}}$$

Visibility

1

0.8

0.6

0.4

0.2

0

Last Scattering Surface

$t_{\rm K} \simeq t_{\rm exp}$

10^2

10^3

10^4

10^5

10^6

10^7

redshift z

y - distortion

μ–*y* transition

μ - distortion

$$y \simeq \frac{1}{4}\frac{\Delta\rho_\gamma}{\rho_\gamma} \equiv \frac{1}{4}\int_0^{z_{\rm K}} \frac{{\rm d}(Q/\rho_\gamma)}{{\rm d}z'}\,{\rm d}z'$$

$$\mu \approx 1.4\int_{z_{\rm K}}^{\infty} \frac{{\rm d}(Q/\rho_\gamma)}{{\rm d}z'}\mathcal{J}_\mu(z'){\rm d}z'$$

$$\mathcal{J}_\mu(z) \approx {\rm e}^{-\left(\frac{z}{2\times10^6}\right)^{5/2}}$$

Visibility

1

0.8

0.6

0.4

0.2

0

Last Scattering Surface

$t_{\rm K} \simeq t_{\rm exp}$

Blackbody fully restored by thermalization

10^2 10^3 10^4 10^5 10^6 10^7

redshift z

y - distortion

μ–*y* transition

μ - distortion

$$y \simeq \frac{1}{4}\frac{\Delta\rho_\gamma}{\rho_\gamma} \equiv \frac{1}{4}\int_0^{z_{\rm K}} \frac{{\rm d}(Q/\rho_\gamma)}{{\rm d}z'}\,{\rm d}z'$$

$$\mu \approx 1.4\int_{z_{\rm K}}^{\infty} \frac{{\rm d}(Q/\rho_\gamma)}{{\rm d}z'}\mathcal{J}_\mu(z'){\rm d}z'$$

$$\mathcal{J}_\mu(z) \approx {\rm e}^{-\left(\frac{z}{2\times10^6}\right)^{5/2}}$$

Visibility

1

0.8

0.6

0.4

0.2

0

Last Scattering Surface

$t_{\rm K} \simeq t_{\rm exp}$

Blackbody "photosphere"

(Bond, Les Houches Lectures, 1996)

10^2 10^3 10^4 10^5 10^6 10^7

redshift z

y - distortion

μ–y transition

μ - distortion

$$y \simeq \frac{1}{4}\frac{\Delta\rho_\gamma}{\rho_\gamma} \equiv \frac{1}{4}\int_0^{z_{\rm K}} \frac{{\rm d}(Q/\rho_\gamma)}{{\rm d}z'}\,{\rm d}z'$$

$$\mu \approx 1.4\int_{z_{\rm K}}^{\infty} \frac{{\rm d}(Q/\rho_\gamma)}{{\rm d}z'}\mathcal{J}_\mu(z'){\rm d}z'$$

$$\mathcal{J}_\mu(z) \approx {\rm e}^{-\left(\frac{z}{2\times10^6}\right)^{5/2}}$$

Very simple way to estimate the spectral distortion for a given energy release history!

Last Scattering Surface

$t_{\rm K} \simeq t_{\rm exp}$

Visibility

redshift z